


 Cite this: *RSC Adv.*, 2021, **11**, 18708

# Inhibition effect of ZrF<sub>4</sub> on UO<sub>2</sub> precipitation in the LiF–BeF<sub>2</sub> molten salt

 Hao Peng,<sup>a</sup> Yulong Song,<sup>ab</sup> Nan Ji,<sup>a</sup> Leidong Xie,<sup>a</sup> Wei Huang<sup>ID</sup>\*<sup>a</sup> and Yu Gong<sup>ID</sup><sup>a</sup>

The dissolution–precipitation behavior of zirconium dioxide (ZrO<sub>2</sub>) in molten lithium fluoride–beryllium fluoride (LiF–BeF<sub>2</sub>, (2 : 1 mol, FLiBe)) eutectic salt at 873 K was studied. The results of the dissolution experiment showed that the saturated solubility of ZrO<sub>2</sub> in the FLiBe melt was 3.84 × 10<sup>−3</sup> mol kg<sup>−1</sup> with equilibrium time of 6 h, and its corresponding apparent solubility product (*K'*<sub>sp</sub>) was 3.40 × 10<sup>−5</sup> mol<sup>3</sup> kg<sup>−3</sup>. The interaction between Zr(IV) and O<sup>2−</sup> was studied by titrating lithium oxide (Li<sub>2</sub>O) into the FLiBe melt containing zirconium tetrafluoride (ZrF<sub>4</sub>), and the concentration of residual Zr(IV) in the melt gradually decreased due to precipitate formation. The precipitate corresponded to ZrO<sub>2</sub>, as confirmed by the stoichiometric ratio and X-ray diffraction analysis. The *K'*<sub>sp</sub> was 3.54 × 10<sup>−5</sup> mol<sup>3</sup> kg<sup>−3</sup>, which was highly consistent with that from the dissolution experiment. The obtained *K'*<sub>sp</sub> of ZrO<sub>2</sub> was in the same order of magnitude as that of uranium dioxide (UO<sub>2</sub>), indicating that a considerable amount of ZrF<sub>4</sub> could inhibit the UO<sub>2</sub> formation when oxide contamination occurred in the melt containing ZrF<sub>4</sub> and uranium tetrafluoride (UF<sub>4</sub>). Further oxide titration in the LiF–BeF<sub>2</sub>–ZrF<sub>4</sub> (5 mol%)–UF<sub>4</sub> (1.2 mol%) system showed that ZrO<sub>2</sub> was formed first with O<sup>2−</sup> addition less than 1 mol kg<sup>−1</sup>, and the precipitation of UO<sub>2</sub> began only after the O<sup>2−</sup> addition reached 1 mol kg<sup>−1</sup> and the precipitation of ZrO<sub>2</sub> decreased the ZrF<sub>4</sub> concentration to 0.72 mol kg<sup>−1</sup> (3 mol%). Lastly, UO<sub>2</sub> and ZrO<sub>2</sub> coprecipitated with further O<sup>2−</sup> addition of more than 1 mol kg<sup>−1</sup>. The preferential formation of ZrO<sub>2</sub> effectively avoided the combination of UF<sub>4</sub> and O<sup>2−</sup>. This study provides a solution for the control of UO<sub>2</sub> precipitation in molten salt reactors.

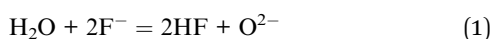
 Received 24th March 2021  
 Accepted 18th May 2021

DOI: 10.1039/d1ra02332b

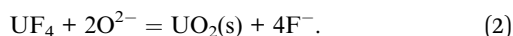
[rsc.li/rsc-advances](http://rsc.li/rsc-advances)

## 1. Introduction

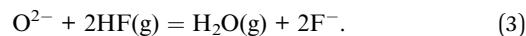
Molten salt reactors (MSRs) use molten fluoride mixtures, usually lithium fluoride–beryllium fluoride mixed melt (LiF–BeF<sub>2</sub> (2 : 1 mol, FLiBe)) as the carrier solvent of fuel, with uranium tetrafluoride (UF<sub>4</sub>) or thorium tetrafluoride (ThF<sub>4</sub>) dissolved as fuel salt.<sup>1–3</sup> However, these fluorides can absorb water due to their hygroscopic nature, and pyrohydrolysis commonly occurs upon melting, thus producing an active oxide impurity (O<sup>2−</sup>) (eqn (1)).<sup>4,5</sup>



Unfortunately, UF<sub>4</sub> has a high sensitivity toward O<sup>2−</sup> in fluoride melts and forms some insoluble compounds of oxides or oxyfluorides,<sup>6</sup> e.g., uranium dioxide (UO<sub>2</sub>) according to our previous investigations (eqn (2)).<sup>7,8</sup>



The large accumulation of the fuel precipitate UO<sub>2</sub> would generate a superheated area in the reactor and cause a criticality risk.<sup>7–11</sup> Hence, the generation of UO<sub>2</sub> in the fuel salt should be strictly controlled to ensure the safe operation of MSR. Two methods have been proposed to protect uranium from UO<sub>2</sub> precipitate formation. One method is to remove the O<sup>2−</sup> impurity in the fuel salt before loaded into the reactor, whereas the other approach is to develop feasible additives to collect O<sup>2−</sup> or facilitate the solubility of UO<sub>2</sub> in molten fluorides during the MSR operation. The Oak Ridge National Laboratory (ORNL) has proposed that bubbling hydrogen fluoride and hydrogen gas (HF/H<sub>2</sub>) mixtures into the salt is an effective means to remove O<sup>2−</sup> (eqn (3)).<sup>12–14</sup>



However, the HF/H<sub>2</sub> purification method has a limited capacity for oxide removal and cannot totally eliminate the O<sup>2−</sup> due to the chemical equilibrium. Moreover, the active oxygen still can be produced through the unexpected nuclear reaction and brought by the cover gas and the external environment.<sup>11,12,15</sup> That means, the residual O<sup>2−</sup> impurity contained in fluorides is inevitable and the formation of UO<sub>2</sub> during the MSR operation remains possible.

<sup>a</sup>Shanghai Institute of Applied Physics, Chinese Academy of Sciences, Shanghai 201800, PR China. E-mail: [huangwei@sinap.ac.cn](mailto:huangwei@sinap.ac.cn); Fax: +86 021 39190136; Tel: +86 021 39190136

<sup>b</sup>University of Chinese Academy of Sciences, Beijing 100049, PR China



Therefore, the development of certain feasible additives to timely collect  $O^{2-}$  or the improvement of the solubility of  $UO_2$  in the molten fluorides is more effective. Zirconium tetrafluoride ( $ZrF_4$ ) may be a good selection, which has a strong affinity toward oxide and is a good oxide getter that can easily capture  $O^{2-}$  to form zirconium oxides (e.g.,  $ZrO_2$ ) or zirconium oxyfluoride species (e.g.,  $ZrOF_2$  and  $Zr_2OF_{10}^{4-}$ ) in the molten fluorides.<sup>16,17</sup> In this manner, the combination of  $U(IV)$  and  $O^{2-}$  can be effectively avoided. Shen *et al.*<sup>16</sup> have studied the interactions between  $Zr(IV)$  and  $O^{2-}$  in lithium fluoride–sodium fluoride–potassium fluoride ( $LiF-NaF-KF$  (46.5 : 11.5 : 42 mol%, FLiNaK)) molten salt and found that different products are formed at different molar ratios of  $nZr(IV)/nO^{2-}$ .  $ZrO_2$  is first formed with  $nZr(IV)/nO^{2-} \leq 0.5$ , and the formed  $ZrO_2$  redissolves into the melt as  $Zr_2OF_{10}^{4-}$  when  $nZr(IV)/nO^{2-} > 0.5$ . These results indicate that the free oxide ions ( $O^{2-}$ ) in the melt can be converted into oxyfluoride complex species ( $Zr_2OF_{10}^{4-}$ ) with enough  $ZrF_4$  additive, which further prevents the  $UO_2$  generation successfully. Besides, Gibilaro<sup>18</sup> has found that the addition of calcium oxide (CaO) into a  $ZrF_4$ -containing lithium fluoride–calcium fluoride ( $LiF-CaF_2$ ) salt leads to the formation of a close to equimolar mixture of solid  $ZrO_2$  and  $ZrO_{1.3}F_{1.4}$ . Korenko *et al.*<sup>19</sup> and our previous studies<sup>7,8,16,20</sup> have used X-ray diffraction (XRD) phase analysis and electrochemical techniques and discovered the  $ZrO_2$  formation when oxide contamination occurs in the  $ZrF_4$ -containing systems (i.e.,  $LiF-NaF-KF-ZrF_4$  and  $LiF-NaF-KF-UF_4-ZrF_4$ ), whereas only  $UO_2$  is observed in the systems without  $ZrF_4$  (i.e.,  $LiF-NaF-KF-UF_4$  and  $LiF-BeF_2-UF_4$ ). These studies demonstrate that  $O^{2-}$  in zirconium-based systems can be reduced by forming  $Zr(IV)$  oxide or oxyfluorides, preventing the  $UO_2$  precipitation.

$ZrF_4$  can also increase the solubility of oxides because of its strong affinity toward oxygen ions. Song *et al.*<sup>21</sup> have studied the dissolution behavior of chromium sesquioxide ( $Cr_2O_3$ ) in various molten fluorides and found that the  $ZrF_4$  additive remarkably increases the solubility of  $Cr_2O_3$  by 19 and 2 times in FLiNaK and FLiBe molten salt, respectively, most likely yielding the dissolution product of  $[ZrO_xF_y]^{4-2x-y}$  complex species. Peng *et al.*<sup>17</sup> have studied the dissolution–precipitation behaviors of  $UO_2$  in molten fluorides and found that  $ZrF_4$  can also improve the solubility of  $UO_2$ . Their results show that the maximum solubility of  $UO_2$  in FLiNaK melt increases by a factor of 5.76 (i.e., increase from 0.247 wt% to 1.422 wt%) when the added  $ZrF_4$  concentration is up to 2.91 wt% and the oxide is dissolved as  $UOF_2$  and  $ZrOF_2$  species. These studies demonstrate that  $ZrF_4$  can easily combine with oxygen ions and form soluble  $Zr(IV)$ -oxyfluorides to improve the solubility of oxides.

From the above,  $ZrF_4$  is probably an ideal additive for controlling the precipitation of  $UO_2$  in molten fluorides. Moreover,  $ZrF_4$  has a low neutron-absorption cross-section, which allows its use in the fuel of MSR. Based on this finding, ORNL<sup>10,11,22</sup> adopts the  $LiF-BeF_2-ZrF_4-UF_4$  (65 : 29.1 : 5 : 0.9 mol%) as the fuel salt of the molten salt reactor experiment, and the use of 5 mol%  $ZrF_4$  successfully raises the oxide tolerance (the maximum allowable amount of  $O^{2-}$  added without the production of  $UO_2$  in the molten salt) to above 100 ppm compared with that of 30 ppm in the molten salt breeder reactor by using a zirconium-free system, i.e.,

$LiF-BeF_2-ThF_4-UF_4$  (71.7 : 16 : 12 : 0.3 mol%). At present, the thorium molten salt reactor-liquid fuel (type 1) (TMSR-LF1) program of China is being launched in the Shanghai Institute of Applied Physics, Chinese Academy of Sciences (SINAP@CAS), which also uses a zirconium-containing system composed of  $LiF-BeF_2-ZrF_4-UF_4$  (65.1 : 28.7 : 5 : 1.2 mol%) as the fuel salt.

In this paper, the dissolution–precipitation behaviors of  $ZrO_2$  and the interactions between  $Zr(IV)$  and  $O^{2-}$  in the FLiBe melt are first studied. Then the apparent solubility product ( $K'_{sp}$ ) of  $ZrO_2$  is obtained and compared with that of  $UO_2$  to predict the generation of oxide precipitations in the fuel salt containing both  $UF_4$  and  $ZrF_4$ . The oxide titration experiment is performed in the FLiBe– $ZrF_4$  (5 mol%)– $UF_4$  (1.2 mol%) system, and the evolutions for the equilibrium concentrations of  $U(IV)$ ,  $Zr(IV)$ , and  $O^{2-}$  with oxide additions are studied to further confirm above theoretical prediction. Finally, the inhibiting effect of  $ZrF_4$  on  $UO_2$  formation is further verified. This study provides an effective solution for controlling and monitoring the nuclear fuel precipitation ( $UO_2$ ) in molten fluorides, which is of great importance for the safe operation of MSR.

## 2. Experimental

### 2.1 Molten salt

The highly purified FLiBe (99.9%) eutectic salt with eutectic temperature of 733 K was prepared and supplied by the SINAP@CAS. The received FLiBe eutectic salt was stored in a glovebox and further dehydrated before use by heating under vacuum from ambient temperature to its melting point for 72 h, to guarantee the high-purity of salt and ensure the reliability of the experiments. During this process, the moisture absorbed by the salt was effectively removed. In order to avoid residual HF remaining in FLiBe, the melt was further purified by sparging the ultra-pure  $H_2$  for 8 h. The FLiBe– $ZrF_4$  and FLiBe– $ZrF_4-UF_4$  melts were thus prepared by artificially adding  $ZrF_4$  (99.99%; Sigma-Aldrich) and  $UF_4$  (99.99%; China North Nuclear Fuel Co., Ltd) to the prepared FLiBe salt.

### 2.2 Experimental method

During the dissolution experiments, the excess of powdery  $ZrO_2$  (ca. 5 g, 99.99%; Sigma-Aldrich) was manufactured into sheets by tableting. The  $ZrO_2$  sheet was dissolved in 50 g FLiBe melt contained in a vitreous carbon crucible, and the saturated

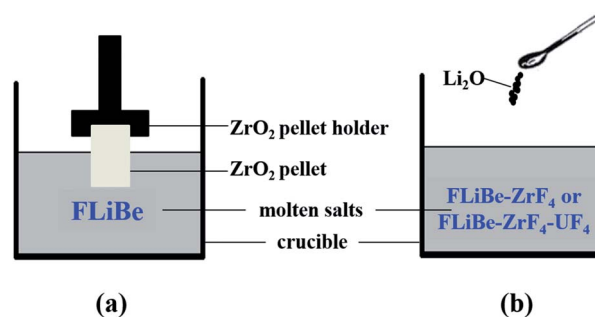


Fig. 1 Schematics of the (a) dissolution and the (b) oxide titration experiments.



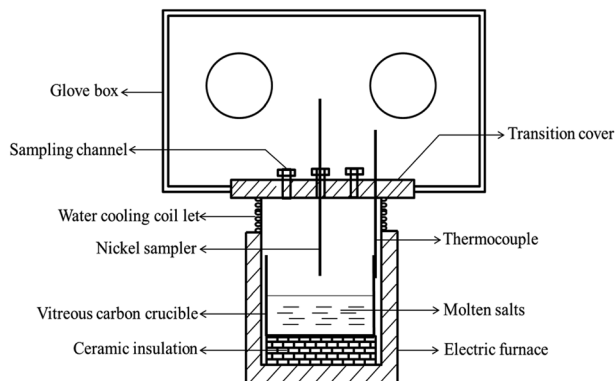


Fig. 2 Schematic of the experimental set-up.

solution of FLiBe–ZrO<sub>2</sub> was formed after equilibrium time. The ZrO<sub>2</sub> sheet was immersed in the salt bath with a graphite pellet holder, as shown in Fig. 1(a). The melt was sampled after the extraction of the pellet from the bath. Thus, no ZrO<sub>2</sub> compound would stick to the sampler, and all the zirconium in the sample was considered to be obtained from ZrO<sub>2</sub> dissolution and could reflect the solubility of ZrO<sub>2</sub>.

During the oxide titration experiments, the oxide ions (O<sup>2-</sup>) were introduced to the FLiBe–ZrF<sub>4</sub> and FLiBe–ZrF<sub>4</sub>–UF<sub>4</sub> baths in the form of lithium oxide (Li<sub>2</sub>O, 99.99%; Sigma-Aldrich), as shown in Fig. 1(b). The interaction between M<sup>(iv)</sup> (M = Zr or U) and O<sup>2-</sup> in the melt would produce ZrO<sub>2</sub> ( $\rho = 5.89 \text{ g cm}^{-3}$ ) or UO<sub>2</sub> ( $\rho = 10.96 \text{ g cm}^{-3}$ ) precipitate and gradually deposit to the bottom of the bath ( $\rho \approx 2 \text{ g cm}^{-3}$ ). When the system reached equilibrium, the supernatant of the molten salt was sampled. The sampling process addressed the use of sintered nickel filter, which prevented the precipitates from sticking to the sampler as proposed by the ORNL,<sup>23</sup> to ensure the accuracy of the experimental results.

The schematic of the experimental apparatus used in present study was shown in Fig. 2, which was described in detail in our previous studies.<sup>7,8,16,17,20,21,24</sup> The whole experiment was conducted in a glove box protected by dry argon atmosphere (99.999%), and the oxygen and water contents in the glove box were both strictly controlled below 0.5 ppm.

### 2.3 Analytical techniques

The oxide concentration in molten fluorides was determined using the LECO oxygen detector (RO600, LECO Co., Ltd)

through the carbothermal reduction technique, which was in accordance with the work of Mediaas<sup>25,26</sup> and our previous studies.<sup>7,8,16,20</sup> Herein, the result measured by LECO was the total oxide content including O<sup>2-</sup> and oxide in oxygenated anions. The oxygenated anions in the melts were determined using ICE ion chromatography (IC, ICS-2100, Dionex Co., Ltd.) with a valve-switching technology.<sup>8</sup>

The concentration of Zr(IV) or U(IV) ions in molten fluorides was determined using inductively coupled plasma optical emission spectroscopy (ICP-OES, Arcos, Spectro Co., Ltd). The detailed testing process has been described previously.<sup>7,8,17</sup> The oxide precipitates formed in molten salt were analyzed using the XRD technique (DY3614, PANzlytical Co., Ltd).

## 3. Results

### 3.1 Concentration of free oxide ions (O<sup>2-</sup>) in molten fluorides

The oxygen in fluoride salt exists in two forms: (i) free oxide ions (O<sup>2-</sup>) and (ii) oxygenated anions (e.g., SO<sub>4</sub><sup>2-</sup>, NO<sub>3</sub><sup>-</sup>, and PO<sub>4</sub><sup>3-</sup>). However, only O<sup>2-</sup> could form oxide precipitates (e.g., UO<sub>2</sub> and ZrO<sub>2</sub>) due to its high sensitivity toward UF<sub>4</sub> and ZrF<sub>4</sub> in molten fluorides. Therefore, the O<sup>2-</sup> concentration in molten fluorides should be measured to clarify the dissolution–precipitation behavior of the fuel salt for MSR. The practical O<sup>2-</sup> concentration ([O<sup>2-</sup>]) in molten fluorides was determined by subtracting the oxide concentration in oxygenated anions ([O]<sub>IC</sub>) from the total oxide concentration ([O]<sub>LECO</sub>), as shown in eqn (4). Table 1 gives the oxide analysis results of two batches of FLiBe melts used in the present study. As shown in Table 1, the total oxygen content of 1# FLiBe was 145 ppm, and the oxygenated anions included NO<sub>3</sub><sup>-</sup>, SO<sub>4</sub><sup>2-</sup>, and PO<sub>4</sub><sup>3-</sup> with content of 83, 55, and 6 ppm, respectively. According to the mass proportion of oxide in the oxygenated anion, the oxide concentrations in NO<sub>3</sub><sup>-</sup>, SO<sub>4</sub><sup>2-</sup>, and PO<sub>4</sub><sup>3-</sup> were 64, 37, and 4 ppm, respectively. Thus, the sum of oxide concentration in these three oxygenated anions were up to 105 ppm, and the O<sup>2-</sup> content was 40 ppm in accordance with eqn (4). Likewise, the O<sup>2-</sup> content of 2# FLiBe was 1383 ppm.

$$[\text{O}^{2-}] = [\text{O}]_{\text{LECO}} - [\text{O}]_{\text{IC}} \quad (4)$$

Table 1 Oxide analysis results of the FLiBe melts used in the present study

Batch number of FLiBe	Total oxide concentration ([O] <sub>LECO</sub> )/ppm	Oxygenated anion concentration/ppm	Oxide in oxygenated anions ([O] <sub>IC</sub> )/ppm	O <sup>2-</sup> concentration ([O <sup>2-</sup> ])/ppm
1# (for oxide titration experiment)	145	NO <sub>3</sub> <sup>-</sup>	83	40 (2.5 × 10 <sup>-3</sup> mol kg <sup>-1</sup> )
		SO <sub>4</sub> <sup>2-</sup>	55	
		PO <sub>4</sub> <sup>3-</sup>	6	
2# (for dissolution experiment)	1500	NO <sub>3</sub> <sup>-</sup>	135	1383 (8.64 × 10 <sup>-2</sup> mol kg <sup>-1</sup> )
		SO <sub>4</sub> <sup>2-</sup>	19	
		PO <sub>4</sub> <sup>3-</sup>	—	



3.2  $K'_{sp}$  of  $ZrO_2$ 

**3.2.1 Dissolution method: FLiBe– $ZrO_2$  system.** The  $ZrO_2$  pellet was immersed into the FLiBe melt to determine the solubility of  $ZrO_2$  in this melt. The melt was sampled at different holding times at 873 K, and the  $Zr(IV)$  concentration in each sample was measured. Fig. 3 gives the plots of  $Zr(IV)$  concentration in the melt versus the dissolution time of  $ZrO_2$ . Apparently, the initial zirconium concentration in the FLiBe melt was below the detection limit of ICP-OES ( $<0.01$  ppm or  $1 \times 10^{-7}$  mol  $kg^{-1}$ ) and could not be detected. When the  $ZrO_2$  was dissolved for the first 2 h, the  $Zr(IV)$  concentration remarkably increased to  $3.37 \times 10^{-3}$  mol  $kg^{-1}$ . Afterwards, the growth rate of  $Zr(IV)$  concentration slowed down, and its value gradually increased to  $3.84 \times 10^{-3}$  mol  $kg^{-1}$  when the dissolution time further increased to 6 h. Then, no remarkable difference was observed in the results of samples collected from 6 h to 22 h, and the  $Zr(IV)$  concentration finally maintained at approximately  $3.84 \times 10^{-3}$  mol  $kg^{-1}$ , which corresponded to the solubility of  $ZrO_2$  with an equilibrium time of 6 h.

In the FLiBe– $ZrO_2$  system, when the dissolution equilibrium of  $ZrO_2$  was achieved, the substances of  $ZrO_2$  compound,  $Zr(IV)$ , and  $O^{2-}$  ions, coexisted and equilibrated, as shown in eqn (5). Thus, the real solubility product ( $K_{sp}$ ) of  $ZrO_2$  could be obtained by multiplying the equilibrium activity of  $Zr(IV)$  ( $a_{Zr(IV)}$ ) and  $O^{2-}$  ( $a_{O^{2-}}$ ), as shown in eqn (6). Actually, a certain deviation existed between the activity ( $a$ ) and the apparent concentration, and this deviation could be quantitatively expressed using the activity coefficient ( $\gamma$ ) with the value less than 1, as shown in eqn (7) and (8). In fact, the  $[Zr(IV)]$  and  $[O^{2-}]$  values obtained by ICP-OES, LECO, and IC techniques were the results of apparent concentrations. Thus, the real solubility product ( $K_{sp}$ ) of  $ZrO_2$  could be calculated through eqn (6), where  $K'_{sp}$  is the apparent solubility product that can be obtained using experimental methods, as shown in eqn (9). However, the measurement of  $a$  and  $\gamma$  ( $\gamma_1$  for  $Zr(IV)$  and  $\gamma_2$  for  $O^{2-}$ , which can be considered as constant in this case) in molten fluorides is a challenging task and leads to a difficult determination of the real  $K_{sp}$ . Nevertheless, the present study only considered the apparent

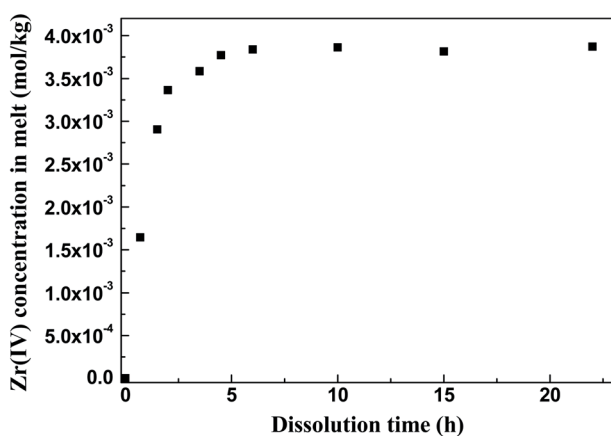
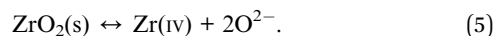


Fig. 3  $Zr(IV)$  concentration versus the dissolution time of  $ZrO_2$  in the FLiBe melt at 873 K.

concentration to deal with this issue, and the  $K'_{sp}$  calculation could also make sense in case of apparent concentration consideration (eqn (9)).



$$K_{sp} = a_{Zr(IV)} \cdot (a_{O^{2-}})^2 = \gamma_1 \gamma_2^2 \cdot [Zr(IV)][O^{2-}]^2 = \gamma_1 \gamma_2^2 \cdot K'_{sp}. \quad (6)$$

$$a_{Zr(IV)} = \gamma_1 \cdot [Zr(IV)]. \quad (7)$$

$$a_{O^{2-}} = \gamma_2 \cdot [O^{2-}]. \quad (8)$$

$$K'_{sp} = [Zr(IV)][O^{2-}]^2. \quad (9)$$

$$[O^{2-}] = [O^{2-}]_{ZrO_2} + [O^{2-}]_{FLiBe}. \quad (10)$$

$$[O^{2-}]_{ZrO_2} = 2[Zr(IV)]. \quad (11)$$

Then, the equilibrium  $[Zr(IV)]$  and  $[O^{2-}]$  were measured to determine the value of  $K'_{sp}$ . In accordance with the solubility of  $ZrO_2$  in FLiBe, as shown in Fig. 3, the equilibrium  $[Zr(IV)]$  in the bath was  $3.84 \times 10^{-3}$  mol  $kg^{-1}$ , whereas the  $O^{2-}$  concentration caused by  $ZrO_2$  dissolution ( $[O^{2-}]_{ZrO_2}$ ) was twice of the  $[Zr(IV)]$ , *i.e.*,  $7.68 \times 10^{-3}$  mol  $kg^{-1}$  (eqn (5) and (11)). Besides, the initial  $O^{2-}$  content in the FLiBe melt ( $[O^{2-}]_{FLiBe}$ ) was  $8.64 \times 10^{-2}$  mol  $kg^{-1}$  (1383 ppm, Table 1). Thus, the equilibrium  $[O^{2-}]$  was  $9.41 \times 10^{-2}$  mol  $kg^{-1}$ , which was obtained using the sum of  $[O^{2-}]_{ZrO_2}$  and  $[O^{2-}]_{FLiBe}$  (eqn (10)). Then, with the obtained values of  $[Zr(IV)]$  and  $[O^{2-}]$ , the  $K'_{sp}$  was calculated to be  $3.40 \times 10^{-5}$  mol<sup>3</sup>  $kg^{-3}$  (eqn (9)).

**3.2.2 Oxide titration method: FLiBe– $ZrF_4$ – $Li_2O$  system.** Oxide ions in the form of  $Li_2O$  were gradually added to the FLiBe– $ZrF_4$  (5 mol%) melt to investigate the interaction between  $Zr(IV)$  and  $O^{2-}$  and its corresponding product. Then, the supernatant melt was sampled after the system reached equilibrium at 873 K, and the  $Zr(IV)$  concentration in each sample was analyzed. Table 2 shows the variation of  $Zr(IV)$  concentration with different oxide additions at 873 K. Apparently, the residual  $Zr(IV)$  concentration in the melt linearly decreased with increasing oxide addition, and the slope of this fitted straight line was 0.51, which approximately equaled to 0.5, as shown in Fig. 4. This result meant a zirconium-containing precipitate with the stoichiometry of  $1Zr^{4+} \cdot 2O^{2-}$ , probably  $ZrO_2$  or  $Zr_xO_{2x}F_y$  species, was formed. Moreover, a kind of white precipitate at the

Table 2 Residual  $Zr(IV)$  and  $O^{2-}$  concentrations in the FLiBe– $ZrF_4$  (5 mol%) melt with different oxide additions, and the variation of calculated  $K'_{sp}$  ( $ZrO_2$ ) value (equilibrium time: 10 h; temperature: 873 K)

Added $O^{2-}$ (mol $kg^{-1}$ )	Equilibrium $[Zr(IV)]$ in melt (mol $kg^{-1}$ )	Equilibrium $[O^{2-}]$ in melt (mol $kg^{-1}$ )	$K'_{sp}$ of $ZrO_2$ (mol <sup>3</sup> $kg^{-3}$ )
0	1.33	—	—
0.11	1.29	$5.20 \times 10^{-3}$ (83 ppm)	$3.49 \times 10^{-5}$
0.16	1.27	$5.29 \times 10^{-3}$ (85 ppm)	$3.55 \times 10^{-5}$
0.26	1.23	$5.43 \times 10^{-3}$ (87 ppm)	$3.63 \times 10^{-5}$
0.34	1.18	$5.48 \times 10^{-3}$ (88 ppm)	$3.54 \times 10^{-5}$
0.47	1.08	$5.71 \times 10^{-3}$ (91 ppm)	$3.52 \times 10^{-5}$

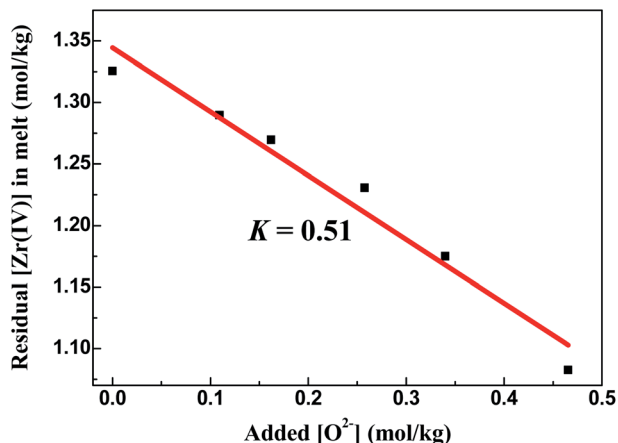


Fig. 4 Linear relationship between the residual [Zr(IV)] and the added  $[O^{2-}]$  in the FLiBe–ZrF<sub>4</sub> (5 mol%) melt at 873 K.

bottom of the melting bath was observed during oxide titration, as shown in Fig. 5(a). To identify the precipitated species, the bottom precipitate was sampled, distilled (to remove the residual matrix salt) and further transferred for XRD analysis.

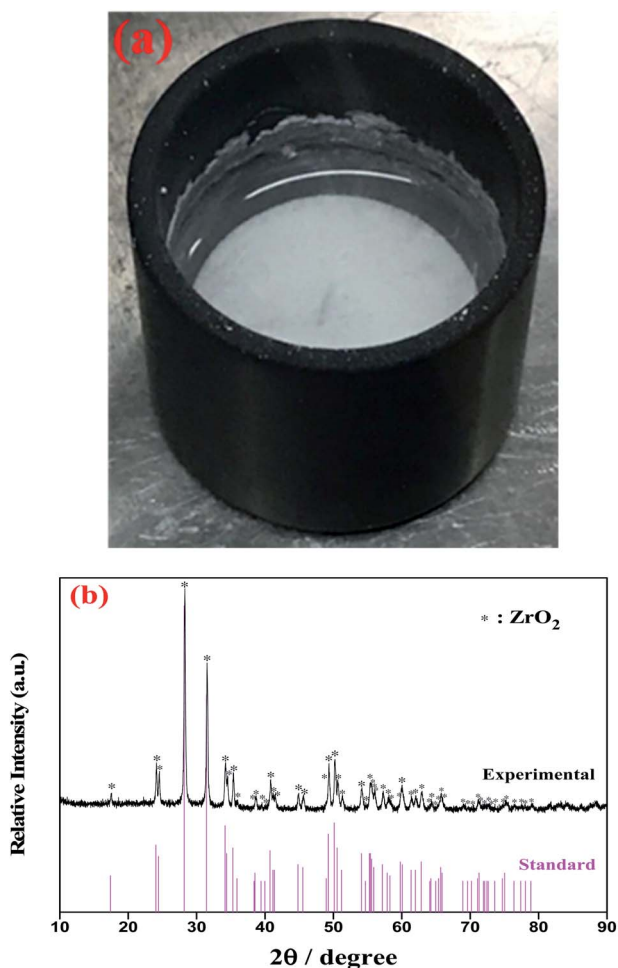


Fig. 5 (a) The observed white precipitate formed at the bottom of the FLiBe–ZrF<sub>4</sub> (5 mol%) melt with  $O^{2-}$  addition at 873 K. (b) XRD pattern of this precipitate obtained after distillation treatment.

The result confirmed that this precipitate corresponded to ZrO<sub>2</sub>, as shown in Fig. 5(b).

With the formation of ZrO<sub>2</sub>, its  $K'_{sp}$  could be calculated by multiplying the equilibrium concentration of  $O^{2-}$  by Zr(IV) (eqn (9)). As shown in Table 2, when the added  $O^{2-}$  increased from 0 mol kg<sup>-1</sup> to 0.47 mol kg<sup>-1</sup>, the remaining Zr(IV) in the melt gradually decreased from 1.33 mol kg<sup>-1</sup> to 1.08 mol kg<sup>-1</sup> whereas the equilibrium  $O^{2-}$  concentration increased from  $5.20 \times 10^{-3}$  mol kg<sup>-1</sup> to  $5.71 \times 10^{-3}$  mol kg<sup>-1</sup>. Thus, a set of  $K'_{sp}$  values were obtained respectively during each oxide addition, and the results located within  $(3.49\text{--}3.63) \times 10^{-5}$  mol<sup>3</sup> kg<sup>-3</sup>. The slight variation in the  $K'_{sp}$  may be attributed to the testing error caused by the chemical analysis. The eqn (9) could be written as:

$$[Zr(IV)] = K'_{sp} \cdot \frac{1}{[O^{2-}]^2}. \quad (12)$$

The linear relationship between the residual [Zr(IV)] and  $1/[O^{2-}]^2$  was fitted (Fig. 6), and the slope of this straight line corresponded to the statistical result of  $K'_{sp}$ . Thus, the final result of  $K'_{sp}$  was determined to be  $3.54 \times 10^{-5}$  mol<sup>3</sup> kg<sup>-3</sup>. This value was highly consistent with that obtained by the dissolution method in FLiBe–ZrO<sub>2</sub> system ( $3.40 \times 10^{-5}$  mol<sup>3</sup> kg<sup>-3</sup>), as stated in Sect. 3.2.1.

### 3.3 Oxide titration to the molten FLiBe–ZrF<sub>4</sub>–UF<sub>4</sub> system

Oxide ions in the form of Li<sub>2</sub>O were gradually added to the FLiBe–ZrF<sub>4</sub> (5 mol%)–UF<sub>4</sub> (1.2 mol%) melt to investigate the inhibiting effect of ZrF<sub>4</sub> on UO<sub>2</sub> formation. Then, the evolutions of the equilibrium concentrations of Zr(IV), U(IV), and  $O^{2-}$  in the melt with oxide addition were determined, and the results could be shown in two stages, as shown in Fig. 7.

**3.3.1 Stage 1: ZrO<sub>2</sub> formation ( $O^{2-}$  addition <1 mol kg<sup>-1</sup>).** The initial Zr(IV) and U(IV) contents of the molten salt were 5 mol% (1.21 mol kg<sup>-1</sup>) and 1.2 mol% (0.28 mol kg<sup>-1</sup>), respectively. Before the added  $O^{2-}$  reached 1 mol kg<sup>-1</sup>, the residual

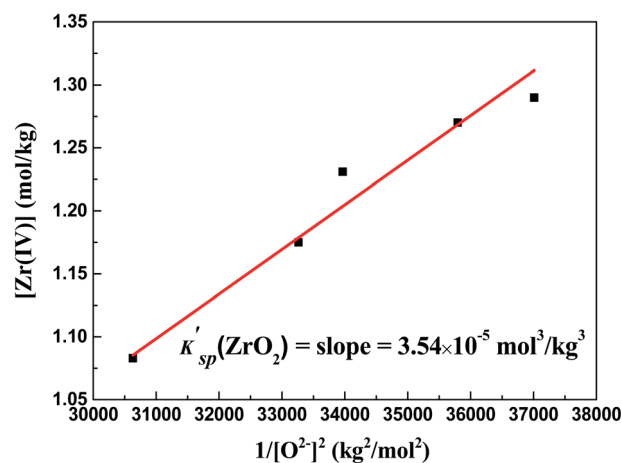


Fig. 6 Determination of  $K'_{sp}$  (ZrO<sub>2</sub>) in the FLiBe–ZrF<sub>4</sub> (5 mol%) melt with  $O^{2-}$  additions at 873 K: linear relationship between the residual [Zr(IV)] and  $1/[O^{2-}]^2$ .



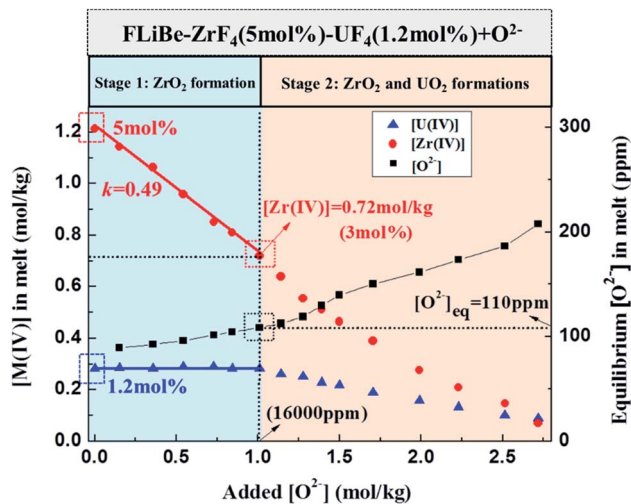


Fig. 7 Evolutions of the equilibrium [Zr(IV)], [U(IV)], and [O<sup>2-</sup>] in the FLiBe-ZrF<sub>4</sub> (5 mol%)-UF<sub>4</sub> (1.2 mol%) melt with oxide additions at 873 K.

Zr(IV) concentration in melt linearly decreased to 0.72 mol kg<sup>-1</sup> and the U(IV) concentration almost remained invariable, whereas the equilibrium O<sup>2-</sup> increased from 90 ppm to 110 ppm. This result indicated that only zirconium-containing precipitate was formed in this period. The slope of the linear relationship between the residual [Zr(IV)] and the added [O<sup>2-</sup>] (0–1 mol kg<sup>-1</sup>) was fitted as 0.49, which approximately equaled to 0.5 (Fig. 7), presuming that insoluble ZrO<sub>2</sub> or Zr<sub>x</sub>O<sub>2x</sub>F<sub>y</sub> species was formed in the melt. Moreover, a kind of white precipitate was observed at the bottom of the bath during experiment, and XRD analysis further proved that this precipitate corresponded to ZrO<sub>2</sub> (Fig. 8). Therefore, only ZrO<sub>2</sub> precipitate was formed with oxide addition less than 1 mol kg<sup>-1</sup>.

**3.3.2 Stage 2: ZrO<sub>2</sub> and UO<sub>2</sub> formations (O<sup>2-</sup> addition ≥ 1 mol kg<sup>-1</sup>).** When the added O<sup>2-</sup> reached 1 mol kg<sup>-1</sup>, the U(IV) concentration drop began, and the equilibrium O<sup>2-</sup> at this time was 110 ppm. When the added O<sup>2-</sup> exceeded 1 mol kg<sup>-1</sup> and reached 2.72 mol kg<sup>-1</sup>, the Zr(IV) and U(IV) in melt were simultaneously consumed and finally decreased to 0.07 and 0.09 mol kg<sup>-1</sup>, respectively. Meanwhile the equilibrium O<sup>2-</sup> further increase to 208 ppm. These results indicated that both zirconium-containing and uranium-containing precipitates were formed in this stage. In addition, the stoichiometry of the total reacted metal ions M(IV) (M = Zr or U) and the added O<sup>2-</sup> was approximately 1 : 2 during this stage. After completion of the experiment, two kinds of precipitates were observed at the bottom of salt. The white one corresponded to ZrO<sub>2</sub> and the rufous one corresponded to UO<sub>2</sub>, as confirmed by XRD (Fig. 8). Therefore, both ZrO<sub>2</sub> and UO<sub>2</sub> were formed with oxide addition more than 1 mol kg<sup>-1</sup>.

## 4. Discussion

### 4.1 K'<sub>sp</sub>: analysis of oxide precipitation behavior in the FLiBe melt

The K'<sub>sp</sub> of ZrO<sub>2</sub> and UO<sub>2</sub> in FLiBe melt were compared to clarify the precipitation law of these two oxides. According to our previous investigation,<sup>8</sup> the K'<sub>sp</sub> (UO<sub>2</sub>) in the FLiBe melt

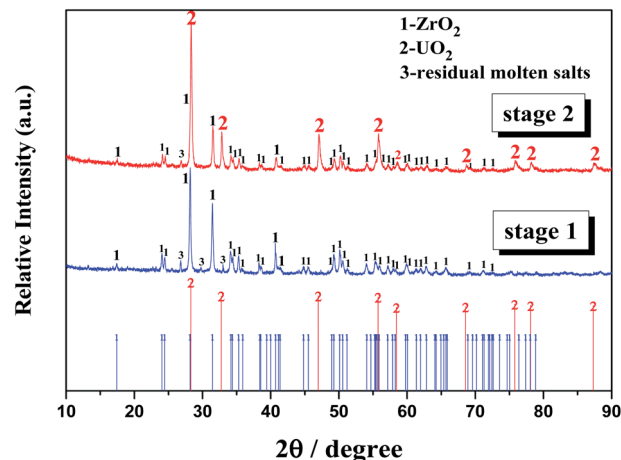


Fig. 8 XRD patterns of the bottom samples obtained in the FLiBe-ZrF<sub>4</sub> (5 mol%)-UF<sub>4</sub> (1.2 mol%) melt with oxide additions after distillation treatment. Stage 1: oxide addition < 1 mol kg<sup>-1</sup>; stage 2: oxide addition > 1 mol kg<sup>-1</sup>.

obtained using the dissolution and the oxide titration methods at 873 K were  $1.67 \times 10^{-5}$  and  $1.33 \times 10^{-5}$  mol<sup>3</sup> kg<sup>-3</sup>, respectively. In this work, the K'<sub>sp</sub> (ZrO<sub>2</sub>) using the dissolution and the oxide titration methods at 873 K were  $3.40 \times 10^{-5}$  and  $3.54 \times 10^{-5}$  mol<sup>3</sup> kg<sup>-3</sup>, respectively. As an equilibrium constant, the K<sub>sp</sub> theoretically depended on temperature only, and the present results also agreed well with those reported by ORNL at the same temperature,<sup>22</sup> as summarized in Table 3.

Evidently, K'<sub>sp</sub> (ZrO<sub>2</sub>) and K'<sub>sp</sub> (UO<sub>2</sub>) were in the same order of 10<sup>-5</sup> mol<sup>3</sup> kg<sup>-3</sup>, and K'<sub>sp</sub> (ZrO<sub>2</sub>) was 2–3 times higher than K'<sub>sp</sub> (UO<sub>2</sub>). Based on these results, we can predict the formation of ZrO<sub>2</sub> and UO<sub>2</sub> precipitates in the FLiBe melt. (i) When the FLiBe melt only contained UF<sub>4</sub>, the reactive oxide resulted in UO<sub>2</sub> precipitation. (ii) When the FLiBe melt contained equimolar ZrF<sub>4</sub> and UF<sub>4</sub>, the oxide contamination should first yield the UO<sub>2</sub> precipitate. (iii) In addition, when the FLiBe melt contained considerably more ZrF<sub>4</sub> than UF<sub>4</sub>, the oxide contamination should first yield the ZrO<sub>2</sub> precipitate. The precipitation of UO<sub>2</sub> began only after the precipitation of ZrO<sub>2</sub> had dropped the ZrF<sub>4</sub> concentration to near 2–3 times as high as that of UF<sub>4</sub>. With further oxide addition, UO<sub>2</sub> and ZrO<sub>2</sub> would precipitate simultaneously. Therefore, excessive ZrF<sub>4</sub> with more than 3 times higher than UF<sub>4</sub> can effectively avoid the formation of UO<sub>2</sub> precipitate in the FLiBe melt.

### 4.2 Oxide precipitation behavior of the MSR fuel salt system FLiBe-ZrF<sub>4</sub>-UF<sub>4</sub>

The oxide titration experiment in the FLiBe-ZrF<sub>4</sub>-UF<sub>4</sub> melt with considerably more ZrF<sub>4</sub> than UF<sub>4</sub> was conducted to validate the above theoretical prediction and further clarify the influence of ZrF<sub>4</sub> on UO<sub>2</sub> generation, as shown in Fig. 7. At first, the ZrF<sub>4</sub> in the system was consumed by forming ZrO<sub>2</sub>, thereby protecting uranium from being precipitated. Until the ZrF<sub>4</sub> concentration dropped to 0.72 mol kg<sup>-1</sup> (3 mol%), precipitation of UO<sub>2</sub> began to form. At this point, the Zr(IV) concentration was about 2.5



Table 3 Comparison between  $K'_{sp}$  (ZrO<sub>2</sub>) and  $K'_{sp}$  (UO<sub>2</sub>) and their ratio  $K'_{sp}$  (ZrO<sub>2</sub>)/ $K'_{sp}$  (UO<sub>2</sub>) ( $k$ ) in the FLiBe melt at 873 K

	$K'_{sp}$ by dissolution method (mol <sup>3</sup> kg <sup>-3</sup> )	$K'_{sp}$ by oxide titration method (mol <sup>3</sup> kg <sup>-3</sup> )	$K_{sp}$ reported by ORNL <sup>22</sup> (mol <sup>3</sup> kg <sup>-3</sup> )
ZrO <sub>2</sub>	$3.40 \times 10^{-5}$	$3.54 \times 10^{-5}$	$3.20 \times 10^{-5}$
UO <sub>2</sub>	$1.67 \times 10^{-5}$ (ref. 8)	$1.33 \times 10^{-5}$ (ref. 8)	$1.20 \times 10^{-5}$
$k$	2.04	2.66	2.67

times as high as that of U(IV). This result was highly consistent with the theoretical prediction, as stated in Sect. 4.1.

With the measured equilibrium concentrations of M(IV) (M = Zr or U) and O<sup>2-</sup>, a set of  $K'_{sp}$  values for ZrO<sub>2</sub> and UO<sub>2</sub> could be respectively obtained after each oxide addition, as shown in Table 4. The  $K'_{sp}$  results were basically consistent with that obtained in the FLiBe melt (Table 3) but varied with O<sup>2-</sup> addition. This was caused by the concentration change of M(IV) in the melt. The  $K'_{sp}$  (ZrO<sub>2</sub>) showed no great difference when the added O<sup>2-</sup> was less than 1.71 mol kg<sup>-1</sup>, but decreased from  $3.45 \times 10^{-5}$  mol<sup>3</sup> kg<sup>-3</sup> to  $1.19 \times 10^{-5}$  mol<sup>3</sup> kg<sup>-3</sup> when the added O<sup>2-</sup> further increased from 1.71 mol kg<sup>-1</sup> to 2.72 mol kg<sup>-1</sup>. At this time, the concentration of Zr(IV) was below 0.39 mol kg<sup>-1</sup>. Whereas the  $K'_{sp}$  (UO<sub>2</sub>) had no remarkable change except some slight fluctuations. The variation of  $K'_{sp}$  (ZrO<sub>2</sub>) probably arose from the deviation between the apparent concentration ( $c$ ) and the activity ( $a$ ) for Zr(IV) in the melt, as shown in eqn (7). The extent of this deviation ( $\gamma \leq 1$ ) was correlated to the concentration of ions.  $\gamma$  increased and decreased when the solute concentration decreased and increased, respectively. In this case, the initial Zr(IV) concentration was about four times greater than the initial U(IV) concentration, and the decrement in [Zr(IV)] varied in a wide range during oxide titration. Thus, when the residual Zr(IV) concentration continued decreasing to a low extent (the added O<sup>2-</sup> was more than 1.71 mol kg<sup>-1</sup> and [Zr(IV)] was below 0.39 mol kg<sup>-1</sup>, which was 1/3 of the initial one), the  $\gamma_1$  for Zr(IV) would increase. Meanwhile, [O<sup>2-</sup>] changed slightly (only about 100 ppm change), indicating that  $\gamma_2$  for O<sup>2-</sup>

remained virtually unchanged. According to eqn (6) and (9), the calculated  $K'_{sp}$  (ZrO<sub>2</sub>) gradually decreased under low [Zr(IV)] when the added O<sup>2-</sup> was more than 1.71 mol kg<sup>-1</sup> and [Zr(IV)] was below 0.39 mol kg<sup>-1</sup>. With regard to U(IV), whose concentration still stayed at a relatively low level, and the decrement occurred on a smaller scale compared with that of Zr(IV). Herein, the  $\gamma_{U(IV)}$  might change slightly, so did the  $\gamma_2$  for O<sup>2-</sup>. Thus, no remarkable variation in  $K'_{sp}$  (UO<sub>2</sub>) was observed in the whole oxide titration procedure.

Fig. 9 illustrates the evolution of  $K'_{sp}$  (ZrO<sub>2</sub>)/ $K'_{sp}$  (UO<sub>2</sub>) ratio ( $k$ ) in the oxide titration duration. The  $k$  value was also equal to the ratio of [Zr(IV)]/[U(IV)] because the O<sup>2-</sup> was simultaneously equilibrated by ZrO<sub>2</sub> and UO<sub>2</sub>, as shown in eqn (13). Apparently,  $K'_{sp}$  (ZrO<sub>2</sub>) was 2.54–1.46 times greater than  $K'_{sp}$  (UO<sub>2</sub>) when the added O<sup>2-</sup> was in the range of 1.01–2.51 mol kg<sup>-1</sup>. However, the difference between them narrowed (decreasing  $k$ ) with oxide addition, and  $K'_{sp}$  (ZrO<sub>2</sub>) <  $K'_{sp}$  (UO<sub>2</sub>) happened when the oxide addition reached 2.72 mol kg<sup>-1</sup> (Fig. 9, bottom X-axis). Meanwhile, the decrease in [Zr(IV)]/[U(IV)] ratio with decreasing uranium concentration was also found (Fig. 9, top X-axis). These results reveal two important information: (i) proposing a solution for monitoring the generation of UO<sub>2</sub> by measuring the  $k$  value in the melt with known [U(IV)]. For example, in this case the FLiBe–ZrF<sub>4</sub> (5 mol%)–UF<sub>4</sub> (1.2 mol%) melt, as long as  $k > 2.5$ , namely the Zr(IV) concentration remains more than 2.5 times that of U(IV), the oxide contamination will not cause UO<sub>2</sub> precipitation; (ii) when [U(IV)] is different, the required [Zr(IV)] (actually, the ratio of [Zr(IV)]/[U(IV)],  $k$ ) which can prevent UO<sub>2</sub>

Table 4 Variation in  $K'_{sp}$  for ZrO<sub>2</sub> and UO<sub>2</sub> in the FLiBe–ZrF<sub>4</sub> (5 mol%)–UF<sub>4</sub> (1.2 mol%) melt with oxide addition at 873 K

Added [O <sup>2-</sup> ] (mol kg <sup>-1</sup> )	[O <sup>2-</sup> ] (mol kg <sup>-1</sup> )	[Zr(IV)] (mol kg <sup>-1</sup> )	[U(IV)] (mol kg <sup>-1</sup> )	$K'_{sp}$ (ZrO <sub>2</sub> ) (mol <sup>3</sup> kg <sup>-3</sup> )	$K'_{sp}$ (UO <sub>2</sub> ) (mol <sup>3</sup> kg <sup>-3</sup> )
0.15	$5.59 \times 10^{-3}$ (89 ppm)	1.14	0.29	$3.57 \times 10^{-5}$	— (no UO <sub>2</sub> formed)
0.36	$5.79 \times 10^{-3}$ (93 ppm)	1.06	0.28	$3.56 \times 10^{-5}$	— (no UO <sub>2</sub> formed)
0.54	$6.01 \times 10^{-3}$ (96 ppm)	0.96	0.29	$3.47 \times 10^{-5}$	— (no UO <sub>2</sub> formed)
0.73	$6.35 \times 10^{-3}$ (102 ppm)	0.85	0.29	$3.43 \times 10^{-5}$	— (no UO <sub>2</sub> formed)
0.84	$6.53 \times 10^{-3}$ (105 ppm)	0.81	0.28	$3.46 \times 10^{-5}$	— (no UO <sub>2</sub> formed)
1.01	$6.80 \times 10^{-3}$ (109 ppm)	0.72	0.28	$3.33 \times 10^{-5}$	$1.31 \times 10^{-5}$
1.14	$7.03 \times 10^{-3}$ (113 ppm)	0.64	0.26	$3.16 \times 10^{-5}$	$1.30 \times 10^{-5}$
1.28	$7.44 \times 10^{-3}$ (119 ppm)	0.55	0.25	$3.07 \times 10^{-5}$	$1.40 \times 10^{-5}$
1.39	$8.10 \times 10^{-3}$ (130 ppm)	0.51	0.23	$3.36 \times 10^{-5}$	$1.50 \times 10^{-5}$
1.50	$8.73 \times 10^{-3}$ (140 ppm)	0.46	0.22	$3.53 \times 10^{-5}$	$1.66 \times 10^{-5}$
1.71	$9.40 \times 10^{-3}$ (150 ppm)	0.39	0.19	$3.45 \times 10^{-5}$	$1.68 \times 10^{-5}$
1.99	$1.01 \times 10^{-2}$ (161 ppm)	0.28	0.16	$2.81 \times 10^{-5}$	$1.61 \times 10^{-5}$
2.23	$1.08 \times 10^{-2}$ (173 ppm)	0.21	0.13	$2.47 \times 10^{-5}$	$1.56 \times 10^{-5}$
2.51	$1.17 \times 10^{-2}$ (186 ppm)	0.15	0.10	$1.99 \times 10^{-5}$	$1.36 \times 10^{-5}$
2.72	$1.30 \times 10^{-2}$ (208 ppm)	0.07	0.09	$1.19 \times 10^{-5}$	$1.50 \times 10^{-5}$



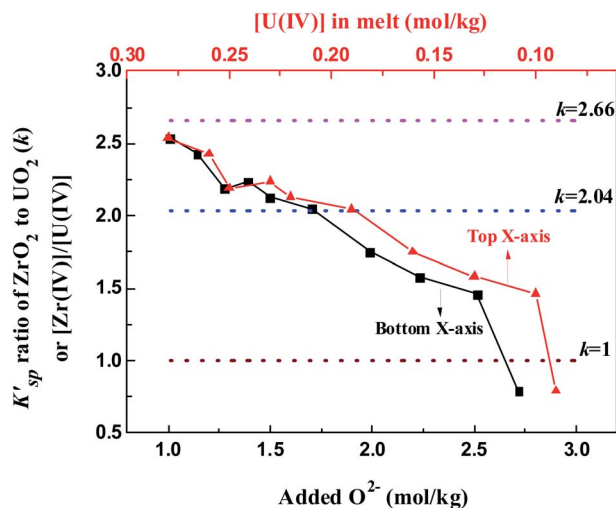


Fig. 9  $K'_{sp}$  ratio of  $ZrO_2$  to  $UO_2$  ( $k$ ) during the oxide titration of FLiBe– $ZrF_4$  (5 mol%)– $UF_4$  (1.2 mol%) melt at 873 K.  $k = 2.66$  obtained by oxide titration method;  $k = 2.04$  obtained by dissolution method;  $k = 1$  means  $K'_{sp}(ZrO_2) = K'_{sp}(UO_2)$ .

precipitation also changes. The lower the  $[U(IV)]$  is, the lower the required  $k$  value will be. For example, when  $[U(IV)]$  is 0.29 mol  $kg^{-1}$ ,  $k \geq 2.5$  is needed to prevent  $UO_2$  precipitation. However, when  $[U(IV)]$  is 0.09 mol  $kg^{-1}$ , it only requires  $k \geq 0.8$ . That means the required  $[Zr(IV)]$  decreased with decreasing  $[U(IV)]$ . These results provide reference data for fuel salt design of MSR with different uranium content.

$$k = \frac{K'_{sp}(ZrO_2)}{K'_{sp}(UO_2)} = \frac{[Zr(IV)][O^{2-}]^2}{[U(IV)][O^{2-}]^2} = \frac{[Zr(IV)]}{[U(IV)]} \quad (13)$$

## 5. Conclusion

The formation of the  $UO_2$  precipitate would lead to a superheated area in MSR and cause a critical risk. Developing appropriate additives for oxide ion capture is an effective way to protect uranium from forming the  $UO_2$  precipitate in the fuel of MSR. This study focused on the dissolution–precipitation behavior of  $ZrO_2$  in the FLiBe melt, and the inhibition of  $UO_2$  generation by the  $ZrF_4$  additive was also clarified.

First, the results of the dissolution experiment showed that the saturated solubility of  $ZrO_2$  in the FLiBe melt at 873 K was 3.84 mol  $kg^{-1}$  with the equilibrium time of 6 h. Then, the interactions between  $Zr(IV)$  and oxide ions was studied by adding  $O^{2-}$  into the FLiBe– $ZrF_4$  melt. The  $Zr(IV)$  concentration in the melt linearly decreased with  $O^{2-}$  addition because of  $ZrO_2$  precipitation, which was confirmed by the stoichiometric ratio (chemical analysis) and XRD. Moreover, the  $K'_{sp}$  of  $ZrO_2$  were determined to be  $3.40 \times 10^{-5}$  and  $3.54 \times 10^{-5}$  mol<sup>3</sup>  $kg^{-3}$  in these two processes, which showed good conformity and were highly consistent with that reported by ORNL.

The obtained  $K'_{sp}$  of  $ZrO_2$  was in the same order of  $10^{-5}$  mol<sup>3</sup>  $kg^{-3}$  and 2–3 times higher than that of  $UO_2$ . Based on this

result, the formation of  $ZrO_2$  and  $UO_2$  precipitates in the FLiBe melt can be predicted. If the FLiBe melt contained considerably more  $ZrF_4$  than  $UF_4$ , the oxide contamination first yielded the  $ZrO_2$  precipitate, and the precipitation of  $UO_2$  began only when the precipitation of  $ZrO_2$  had dropped the  $ZrF_4$  concentration to near 2–3 times as high as that of  $UF_4$ . The oxide titration experiment of the FLiBe– $ZrF_4$  (5 mol%)– $UF_4$  (1.2 mol%) melt was further carried out, showing that only  $ZrO_2$  was formed when the  $O^{2-}$  addition was less than 1 mol  $kg^{-1}$ . When the added  $O^{2-}$  reached 1 mol  $kg^{-1}$  and the  $[Zr(IV)]$  reduced to 0.72 mol  $kg^{-1}$  (3 mol%),  $UO_2$  began to form and the  $[Zr(IV)]/[U(IV)]$  ratio was 2.5 at this point. Afterwards,  $ZrO_2$  and  $UO_2$  coprecipitated with further  $O^{2-}$  addition. Experimental results agreed well with the theoretical prediction from the obtained  $K'_{sp}(ZrO_2)$  and  $K'_{sp}(UO_2)$ .

The results of present work clarified the inhibiting effect of  $ZrF_4$  on the  $UO_2$  generation in the FLiBe melt and further affirmed the approach of  $ZrF_4$  additive for the control of nuclear fuel precipitation ( $UO_2$ ) in MSR. When oxide contamination occurred, the considerable amount of  $ZrF_4$  first formed  $ZrO_2$ , which prevented the combination between  $UF_4$  and  $O^{2-}$ . Thus, the precipitation of  $UO_2$  could be effectively avoided. The critical ratio of  $[Zr(IV)]/[U(IV)]$  to prevent the precipitation of  $UO_2$  was more than 2.5 in the FLiBe– $ZrF_4$  (5 mol%)– $UF_4$  (1.2 mol%) melt, and it decreased with decreasing initial uranium concentration. The precipitation mechanism of  $ZrO_2$  and  $UO_2$  in the FLiBe molten salt can provide the following inspirations: (i) a solution for monitoring the generation of  $UO_2$  precipitation in the MSR fuel salt can be proposed by measuring the  $[Zr(IV)]$ ; (ii) the required  $[Zr(IV)]/[U(IV)]$  ratio which can prevent  $UO_2$  precipitation changes with different uranium content. All of these will be helpful for the safe operation and fuel salt design of MSR.

## Conflicts of interest

There are no conflicts to declare.

## Acknowledgements

This work was supported by the National Natural Science Foundation of China (Grant No. 22006150), Shanghai Sailing Program (Grant No. 19YF1458200), “Strategic Priority Research Program” and the “Frontier Science Key Program” of the Chinese Academy of Sciences (Grant No. XDA02030000 and QYZDYSSW-JSC016).

## References

- M. Rosenthal, P. Kasten and R. Briggs, Molten-salt reactors: history, status, and potential, *Nucl. Appl. Technol.*, 1970, **8**, 107–117.
- W. R. Grimes, F. F. Blankenship, G. W. Keilholtz, H. F. Poppendiek and M. T. Robinson, Chemical aspects of molten fluoride reactors, in *Progress in Nuclear Energy, Series IV*, Pergamon Press, London, 1960, vol. 2.



- 3 A. Nuttin, D. Heuer, A. Billebaud, R. Brissot, C. Le Brun, E. Liatard, J.-M. Loiseaux, L. Mathieu, O. Meplan and E. Merle-Lucotte, Potential of thorium molten salt reactors: detailed calculations and concept evolution with a view to large scale energy production, *Prog. Nucl. Energy*, 2005, **46**, 77–99.
- 4 F. Lantelme and H. Groult, *Molten Salts Chemistry: from Lab to Applications*, Elsevier, 2013.
- 5 S. Delpech, C. Cabet, C. Slim and G. S. Picard, Molten fluorides for nuclear applications, *Mater. Today*, 2010, **13**, 34–41.
- 6 P. A. Haas and P. Cooper, Solubility of uranium oxides in fluoride salts at 1200 °C, *J. Chem. Eng. Data*, 1993, **38**, 26–30.
- 7 H. Peng, M. Shen, Y. Zuo, X. X. Tang, R. Tang and L. D. Xie, Electrochemical technique for detecting the formation of uranium-containing precipitates in molten fluorides, *Electrochim. Acta*, 2016, **222**, 1528–1537.
- 8 H. Peng, W. Huang, L. D. Xie and Q. N. Li, Solubility and precipitation investigations of UO<sub>2</sub> in LiF–BeF<sub>2</sub> molten salt, *J. Nucl. Mater.*, 2020, **531**, 152004.
- 9 ORNL-3812, *Molten-salt Reactor Program: Semiannual Progress Report for Period Ending*, Oak Ridge National Laboratory, 1965.
- 10 ORNL-3936, *Molten-salt Reactor Program: Semiannual Progress Report for Period Ending*, Oak Ridge National Laboratory, 1966.
- 11 ORNL-4812, *Molten-salt Reactor Program: the Development Status of Molten-Salt Breeder Reactors*, Oak Ridge National Laboratory, 1972.
- 12 ORNL-3708, *Molten-salt Reactor Program: Semiannual Progress Report for Period Ending*, Oak Ridge National Laboratory, 1964.
- 13 ORNL-4616, *Reactor Chemistry Division: Preparation and Handling of Salt Mixtures for the Molten Salt Reactor experiment*, Oak Ridge National Laboratory, 1971.
- 14 A. L. Mathews and C. F. Baes Jr., Oxide chemistry and thermodynamics of molten lithium fluoride-beryllium fluoride solutions, *Inorg. Chem.*, 1968, **7**, 373–382.
- 15 ORNL-TM-0728, *report, MSRE Design and Operations Report: Part I. Description of Reactor Design*, Oak Ridge National Laboratory, 1965.
- 16 M. Shen, H. Peng, M. Ge, C. Y. Wang, Y. Zuo and L. D. Xie, Chemical interactions between zirconium and free oxide in molten fluorides, *RSC Adv.*, 2015, **5**, 40708–40713.
- 17 H. Peng, M. Shen, Y. Zuo, H. Y. Fu and L. D. Xie, Chemical and electrochemical studies on the solubility of UO<sub>2</sub> in molten FLINAK with ZrF<sub>4</sub> additive, *J. Nucl. Mater.*, 2018, **510**, 256–264.
- 18 M. Gibilaro, L. Massot, P. Chamelot, L. Cassayre and P. Taxil, Investigation of Zr(IV) in LiF–CaF<sub>2</sub>: stability with oxide ions and electroreduction pathway on inert and reactive electrodes, *Electrochim. Acta*, 2013, **95**, 185–191.
- 19 M. Korenko, M. Straka, J. Uhlíř, L. Szatmáry, M. Ambrová and M. Šimurda, Phase analysis of the solidified KF–(LiF–NaF–UF<sub>4</sub>)–ZrF<sub>4</sub> molten electrolytes for the electrowinning of uranium, *J. Radioanal. Nucl. Chem.*, 2014, **302**, 549–554.
- 20 M. Shen, H. Peng, M. Ge, Y. Zuo and L. D. Xie, Use of square wave voltammeter for online monitoring of O<sup>2–</sup> concentration in molten fluorides at 600 °C, *J. Electroanal. Chem.*, 2015, **748**, 34–39.
- 21 Y. L. Song, M. Shen, H. Peng, C. Y. Wang, S. F. Zhao, Y. Zuo and L. D. Xie, Solubility of Cr<sub>2</sub>O<sub>3</sub> in Molten Fluorides with Different ZrF<sub>4</sub> Contents and Fluoroacidities, *J. Electrochem. Soc.*, 2020, **167**, 023501.
- 22 ORNL-3419, *Molten-salt Reactor Program: Semiannual Progress Report for Period Ending*, Oak Ridge National Laboratory, 1963.
- 23 ORNL-1771, *Aircraft Nuclear Propulsion Project: Quarterly Progress Report for Period Ending*, Oak Ridge National Laboratory, 1954.
- 24 H. Peng, M. Shen, C. Y. Wang, T. Su, Y. Zuo and L. D. Xie, Electrochemical investigation of the stable chromium species in molten FLINAK, *RSC Adv.*, 2015, **5**, 76689–76695.
- 25 H. Mediaas, J. Vinstad and T. Østvold, *Solubility of MgO in MgCl<sub>2</sub>–NaCl–NaF Melts*, Minerals, Metals and Materials Society, Warrendale, PA (United States), 1996.
- 26 G. Kipouros, H. Mediaas, J. Vinstad, T. Østvold and O. Tkatcheva, *Oxide Solubilities and Phase Relations in the System Mg–Nd–O–Cl*, Minerals, Metals and Materials Society, Warrendale, PA (United States), 1996.

